Switching the Interpenetration of Confined Asymmetric Polymer Brushes.

DOI:
10.1021/acs.macromol.6b00310

Document Version
Accepted author manuscript

Switching the Interpenetration of Confined Asymmetric Polymer Brushes.

Stephen B. Abbott,[a,b] Wiebe M. de Vos,[*,c] Laura L. E. Mears,[a] Maximilian Skoda,[d] Robert Dalgliesh,[d] Steve Edmondson,[e] Robert M. Richardson,[a] Stuart W. Prescott[b,f]

[a] *School of Physics, University of Bristol, BS8 1TL, UK*

[b] *School of Chemistry, University of Bristol, BS8 1TS, UK*

[c] *Membrane Science and Technology, Mesa+ Institute for Nanotechnology ,University of Twente, 7500 AE Enschede, Netherlands*

[d] *ISIS facility, Rutherford-Appleton Laboratory, Chilton, Didcot, Oxon, OX11 0QX ,UK*

[e] *School of Materials, The University of Manchester, Oxford Road, Manchester, M13 9PL, UK*

[f] *School of Chemical Engineering, UNSW Australia, Sydney NSW 2052, Australia*

[*]Corresponding Author: w.m.devos@utwente.nl

Abstract

The interpenetration of two polymer brushes on approaching flat surfaces has been investigated. When compacting polymer brushes with an asymmetric charge on each surface, one neutral and the other weakly charged, we find that the brush interpenetration becomes a parameter that can be controlled by the pH of the hydrating solution. The switching between high and low degrees of brush interpenetration was investigated with numerical self-consistent field theory (nSCF) and experimentally using a sample environment which combines neutron reflectometry with a surface force type apparatus. Initially, a pair of uncharged poly(ethylene oxide), PEO, brushes are examined, where one of the brushes is

deuterated to distinguish it from a hydrogenous counter-part. We find in both nSCF and these experiments that there is no significant overlap between the brushes as both compact into polymer blocks with little hydration. However, when a weak polyelectrolyte poly(2-(dimethylamino)ethyl methacrylate), PDMAEMA, brush is confined against a deuterated neutral PEO brush and the pH of the hydrating solution is below the polycation's pK_a of 7.5, then the presence of charged groups on the PDMAEMA allows significant interpenetration to occur between the two polymer brushes on contact. This interpenetration remains once the polymer brushes dehydrate due to the confining pressure that is applied. Raising the pH to a value above the pK_a, removes the charges from the polyelectrolyte brush resulting in little to no interpenetration between the two brushes. Therefore, by simply adjusting the pH of the hydrating solution the interpenetration state between polymer brush pairs can be switched when one brush is a weak polyelectrolyte. Since polymer brushes are widely investigated and used to reduce friction between solid surfaces, this effect may have significant implications in the design and operation of polymer brushes with controllable friction properties.

Introduction

The physics of adhesion, lubrication, and friction are determined by the forces of interaction between two surfaces. These forces can be controlled by coating a surface with a polymer brush,[1,2] a highly dense array of polymer chains grafted at one end to a surface to form a carpet-like structure. One very promising application of the polymer brush is to reduce friction. Coating two surfaces with polymer brushes has been shown on many occasions to significantly (by orders of magnitude) reduce the friction relative to bare surfaces.[3,4] The key to this behaviour is believed to be that even under moderate compression of the brush layers, there is almost no interpenetration between the brushes, leaving a low viscosity interfacial fluid layer where shear

can take place easily.[5,6] If one could therefore control the interpenetration between the two polymer brushes, by for example changing the solution pH, one could manipulate the friction between interfaces.

For both neutral polymer brushes and charged polymer brushes, very low coefficients of friction have been observed, indicating very low levels of interpenetration.[5–7] This is explained by the polymer in a neutral brush stretching to reduce the high polymer density, just as the polymer in a charged brush stretches to reduce its high charge density. However, if either uncharged or charged brushes come into contact with a similarly charged brush, stretching and thus penetrating into the other brush is unfavourable, as it would neither reduce the polymer nor the charge density. Therefore, the brushes compact with little to no interpenetration resulting in the low friction surfaces reported. Here polyelectrolyte brushes are especially interesting as they can withstand high confining pressures with relatively low overlap due to additional osmotic pressure from the counterions.[8,9]

There are good reasons to believe however, that compressing a charged brush against a neutral brush would show a large amount of interpenetration. As the charged brush is pushed against a neutral polymer brush, stretching and subsequent interpenetration still reduces the charge density in the polyelectrolyte brush, and reduces the high polymer density in the neutral brush. Thus interpenetration between the brushes would be favourable. Further extending this concept by having one of the brushes weakly charged, thus being able to switch between a symmetric state (both brushes uncharged) to an asymmetric state (one charged brush and another uncharged), would allow for a simple method to switch between high and low brush interpenetration.

A technique that is sensitive enough to demonstrate this switch between high and low brush interpenetration is neutron reflectometry. This technique has been used to experimentally confirm the predicted parabolic like volume fraction profile of a polymer brush.[10,11] However, most previous experimental attempts to determine the structure of two interacting brushes under complete confinement have proven difficult. This is a consequence of the complications involved in bringing two solid surfaces together over a sufficient surface area for neutron reflection. Typically, using silicon and quartz substrates, confinement less than 80 nm has not been achieved due to the inherent, long range, waviness of the substrates and the difficulty of keeping dust out of the beam footprint area, as demonstrated by Cosgrove et al.[12] Alternative methods of investigating the interaction between two polymer brushes, such as using colloid probe AFM (for example, the work of Pasche et al.[13]), does not yield direct information about the structure of the polymer brushes whilst they are compressed together. In thin polymer films confinement can also be achieved by anchoring one species of polymer to the air-polymer interface,[14,15] but unfortunately this approach cannot be used in the presence of a solvent.

More recently, Kuhl and co-workers[12,13] have been able to partially overcome these limitations by using dense, long brushes approximately 80 nm thick. Confinement was achieved by using another polymer brush layer of similar thickness to bridge the confinement gap between the two solid surfaces and to determine the interaction between the brushes. This work demonstrated that pairs of polystyrene brushes compress under confinement, increasing the polymer density throughout the brush, including near the grafting surface. However, this approach only works for specific polymers with very long brush lengths; here, the chemistry of interest requires the use of much thinner brush layers.

The limitations on bringing two surfaces into direct contact has recently been overcome by using an apparatus combining a surface force type device for use with neutron reflectometry using a flexible thin polymer sheet.[18] A pneumatic pressure was used to deflect the sheet and to control the confinement force. By using a flexible sheet approach, instead of using two solid surfaces to provide confinement, one surface is able to deform over any unintended trapped dust particles or long range surface roughness associated with the solid substrate. This apparatus has made it possible to study the effect of confinement on the structure of thin polymer films,[18–20] including polymer brush layers,[21] allowing a clear explanation of measured surface forces.

In this article, the structure of two polymer brushes pressed into direct contact with each other in an aqueous environment is considered. The confined brushes are asymmetric, with one brush being uncharged poly(ethylene oxide) and the other being a weak polycation, poly(2-(dimethylamino)ethyl methacrylate) (PDMAEMA). Initially, numerical self-consistent field theory (nSCF) is used to examine the effect of charging the brushes. These predictions are then compared to experimental data acquired using the flexible polymer sheet apparatus. The data demonstrate the first example of a system where the interpenetration between polymer brushes can be controlled by simply changing the pH.

Numerical self-consistent field theory simulations

A very successful approach in theoretically predicting the structure or density profiles of two confined polymer brushes is numerical self-consistent field (nSCF) theory. This approach has on many occasions shown excellent agreement with experimentally determined density profiles[22] and with molecular dynamics simulations,[23] while being computationally many orders of magnitude more efficient. Therefore, the nSCF lattice model of Scheutjens and Fleer is

implemented, of which excellent descriptions are readily available in the literature.[24–26] Only the essential theory and assumptions used in this model are discussed here.

To accurately simulate polymer brushes it is necessary to solve the Edwards diffusion equation for polymer chains in inhomogeneous systems[27]

$$\frac{\partial G(\mathbf{r}, s \mid 1,1)}{\partial s} = \left(\frac{1}{6} \nabla^2 - u(\mathbf{r}) \right) G(\mathbf{r}, s \mid 1,1) \qquad (1)$$

where the Green's function G represents the statistical weight of all possible conformations of polymer chains with segment $s' = 1$, next to the surface ($\mathbf{r}_z = 1$) and segment $s' = s$ at coordinate $\mathbf{r}$. This quantity is closely related to the chain partition function (that is, when $s = N$) and hence to the free energy of the system. In eq.1, it is necessary to specify the dimensionless segment potential $u(\mathbf{r})$. The role of the segment potential is to mimic excluded-volume interactions. This potential also accounts for the solvent quality. In these simulations, it is assumed that there is only one relevant coordinate, namely the distance to the grafting interface (z-coordinate). In this case the segment potential becomes self-consistent when $u(z) = v\varphi(z)$, with φ the volume fraction of polymer, and v the segment volume. A polymer chain should connect its free end, irrespective of the z-position of this (free) end, to the grafting segment by taking N steps in this potential field. The system can realize this by insisting on a parabolic shape of the segment potential, that is $u(z) = A - Bz^2$. The parabolic potential is the basis for many analytical SCF models and directly leads, for good solvent conditions, to the well-known parabolic volume fraction profile for a dense brush where the chains are strongly stretched.[28,29] However, in our numerical SCF model, no prior assumptions are made considering the shape of the segment potential. This is especially relevant as under confinement and in contact with another brush a parabolic density profile is not expected.

To study the confinement of charged polymer brushes, an important extra term in the dimensionless segment potential is required, namely $\Psi(z) = e\psi(z)/kT$, where e is the elementary charge and $\psi(z)$ is the electrostatic potential. To evaluate this electrostatic potential one needs to solve the Poisson equation:[30]

$$\nabla^2\Psi(z) = -\lambda_B q(z) \qquad (2)$$

Here, $q(z)$ is the number distribution of charges, where cations add positively and anions negatively to this quantity, and λ_B is the Bjerrum length which in water, around room temperature, is approximately 0.7 nm. It is assumed that the dielectric permittivity is equal to that of water throughout the system. The presence of charged segments in the brush introduces an electrostatic contribution to the effective virial coefficient. This contribution is inversely proportional to the concentration of mobile salt ions, φ_s, and a quadratic function of the charge density α in the brush:[31] $v_{el} = \alpha^2/\varphi_s$. In many cases, the virial coefficient is negligible compared to the electrostatic contribution.

For weak polyelectrolytes such as PDMAEMA, the charge or degree of dissociation will depend on the pH, the ionic strength and on the local electrostatic potential. This is modelled by a two state model.[27] For a weakly charged polycation, the basic monomer B comes in two states, a deprotonated state with neutral charge and a protonated state which is positive: $B + H_2O = B^+ + OH^-$. For PDMAEMA we assume a monomeric pK_a value of 7.5.[33,34]. The auto-dissociation of water is implemented as $2H_2O = OH^- + H_3O^+$ with a pK_w of 14. The degree of protonation, α, at location z then follows from: $\alpha(z) = \frac{K_a}{K_a + [H^+]e^{-y(z)}}$, where y(z) represents the local electrostatic potential.

As a result, the density profile of a weakly charged brush can deviate from the parabolic profile typically assumed in a-SCF models. Especially at low ionic strength, the degree of

association (positive charge) deep inside the brush will be much lower compared to the degree of association at the edge of the brush.[35] This is the result of the local electrostatic potential being significantly different between these two locations and leads to substantial deviations from the parabolic density profile. However, an increase in the ionic strength leads to a more uniform distribution in the degree of dissociation and the density profile reassumes its parabolic shape.

Here we described two surfaces, separated by a distance of 60 lattice sites that are both decorated with a brush, on one surface the brush is neutral while on the other surface the brush is a weak polybase. Apart from the difference in charge, the brushes are identical, with a chain length of 100 monomers, and grafting density of 0.025 chain per lattice site (or 0.28 chains per nm^2). This set of parameters makes sure that we are well within the brush regime for both brushes, using experimentally relevant conditions. We do not go higher in chain length than a 100 monomers to allow for faster computation. By keeping the two polymer brushes identical, except for their charge, we can see the effect of charge on interpenetration most clearly. Both polymers (and all ions) are in good solvent conditions (χ_s = 0) and do not show enthalpic interaction with each other (χ_{ab} = 0). The spacing of a lattice site is set at 0.3 nm in all dimensions. The chosen lattice size spacing also sets the step size of the freely jointed chain model used to describe the polymer chains. Furthermore, we assume incompressibility and implement this by not allowing free lattice sites (every lattice site is occupied). The confined brushes under investigation are in equilibrium with a solvent reservoir. This means that the solvent can freely exchange with a bulk and therefore the number of solvent molecules in the brush depend on the confinement.

As mentioned, for our weakly charged polymer PDMAEMA we assume a monomeric pK_a value of 7.5.[33,34] However, for charged brushes, it is also essential to set a bulk ionic strength,

which in this case is set at φ_s = 0.001, where φ_s is the volume fraction of salt ions. This corresponds to an ionic strength of about 50 mM.

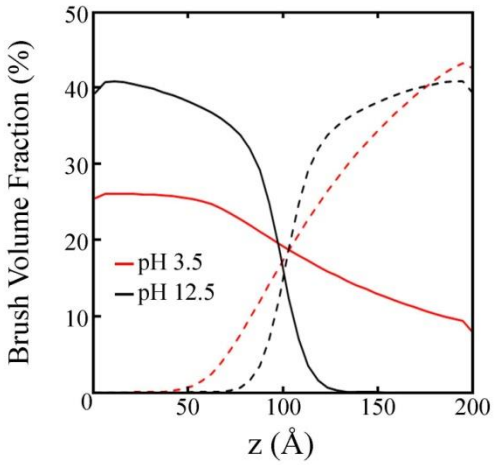

Figure 1: Theoretical brush volume fractions determined by nSCF for two brushes of equal chain length and grafting density. The polycationic brush is on the left side (solid line), while the neutral brush is on the right (dashed line).

With these parameters, and using the discretization scheme of Scheutjens and Fleer,[24] we solve equations 1 and 2 to obtain the density profiles of both the neutral and the polybasic brush. At a high pH of 12.5 the polybasic brush is uncharged, and when we subsequently confine the two polymer brushes we find, as expected, only a very low degree of interpenetration, see Figure 1, pH 12.5. The brushes simply compact against each other into a polymer block with a higher density than the brushes had before compression. The small overlap region in the volume fraction profiles is a result of entropy, as the final parts of the brush are hardly stretched, they can still gain entropy by mixing.

However, at low pH, when the polybasic brush is highly charged steric repulsion between the two brushes is no longer as effective in preventing interpenetration (figure 1, pH 3.5). Bringing together the charged and the uncharged brush leads to a great deal of overlap in the volume fraction profiles and also demonstrates very asymmetric behaviour between the two brushes. The charged polymer chains stretch strongly to lower the electrostatic repulsion (or the resulting osmotic pressure of the counter ions) as much as possible and the neutral polymer chains are thus used to "dilute" the charged monomers and their counter ions.

For pH 3.5, we further find (data not shown) that the density profile of counter ions (Cl^-) is essentially equal to the density profile of the charged polymer. This demonstrates that the chain is indeed fully charged, but also that in this confined state the monomeric charges are spread out substantially enough that every location (z) is essentially charge neutral. This strengthens the hypothesis that it is the osmotic pressure of the counter-ions that leads to the substantial swelling (even under confinement) and thus mixing of the charged and uncharged brushes.

For the neutral brush we predict that the change in conformation is much smaller than the charged brush, and is simply a result of the penetration of the charged monomers. As a result of the charges in the brush, more solvent is retained within the charged brush.

So far we have focussed on two extreme cases, but in figure 2 we demonstrate that as a function of pH there is a gradual transition from low to high interpenetration occurring around the brush pK_a (between pH 6.5 and 9.5). Here interpenetration is defined as $I = \int_0^{zmax} \varphi_a \varphi_b$, which is zero when there is no overlap, but becomes very substantial when you have a high volume fraction of the two species ($\varphi_a \varphi_b$) in the same location. Below pH 6 the polybasic brush is fully charged and we find a constant and significant overlap between the volume fraction profiles of the brushes. Above pH 10 the polybasic brush is uncharged and a constant very low

degree of interpenetration is found. Our simulations thus clearly confirm that in the proposed asymmetric brush system, consisting of a neutral and a polybasic brush, the brush interpenetration becomes a tuneable parameter. For polyanion brushes, the first and last regions would switch position and the transition region would shift according to the pK_a.

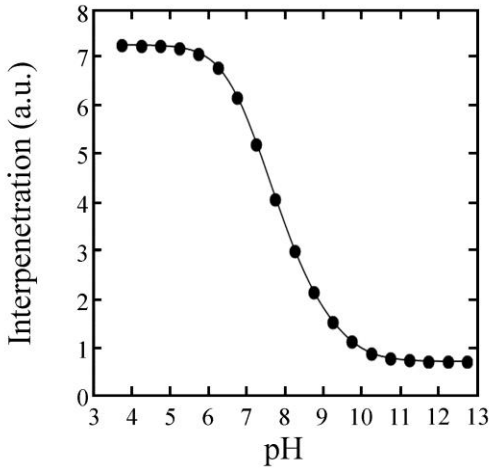

Figure 2: Theoretical brush interpenetration determined by nSCF as the pH of the hydrating solution is varied.

Experimental Methods

Materials: Vinyl terminated polystyrene, vPS (M_w = 1,700 and 19,000), deuterated polystyrene, dPS (M_w = 723,700, d-8), the deuterated diblock-copolymer dPS-dPEO (M_w = 4,800-co-18,500), and diblock-copolymer PS-PEO (M_w = 3,600-co-16,600) were acquired from Polymer Source Inc.

The toluene (99.8%) and chloroform (>99.9%, HPLC grade) used to make various solutions of the polymers was purchased from Sigma-Aldrich.

The substrates used were silicon blocks of 76.3 mm diameter and 10 mm thickness with the top side polished; these were purchased from Crystran Ltd., UK.

Demineralised (Milli-Q) water with a resistivity of 18.2 MΩcm was used in experiments to hydrate the PEO polymer brushes. For the PDMAEMA brush hydration, a solution with a background ionic strength of 1mM NaCl was used, while the pH was set using HCl and/or NaOH immediately prior to the measurements.

The flexible membrane is a sheet of poly (ethylene terephthalate), 'Melinex', 50 μm in thickness. This was supplied by DuPont-Teijin films.

For PDMAEMA brush growth, 2-(dimethylamino)ethyl-methacrylate (DMAEMA, 98% containing 700-1000 ppm monomethyl ether hydroquinone as inhibitor), $CuBr_2$ (99%), ascorbic acid (≥ 99%), 1,1,4,7,10,10-hexamethyltriethylenetetramine (HMTETA, 97%), propan-2-ol (LR grade, ≥ 99.5%) and acetone (LR grade, ≥ 99.5%) were purchased from Sigma-Aldrich. Water was demineralised (18.2 MΩcm) using an Elga Option 4 system. Each 30 ml portion of DMAEMA monomer was passed through a ~5 cm column of alumina (activated, neutral, Brockmann I, Sigma-Aldrich) to remove inhibitor and used immediately.

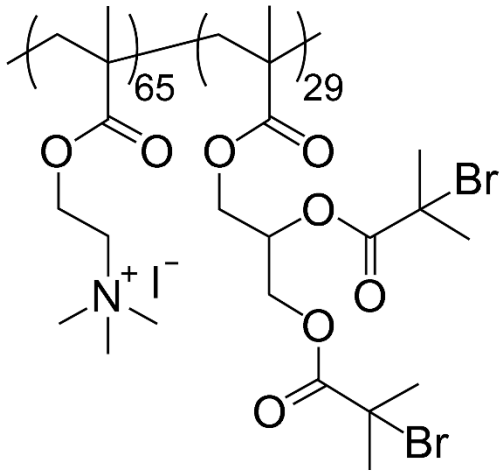

Figure 3: Chemical structure of the macroinitiator.

The cationic macroinitiator, with structure given above, was synthesised from 2-(dimethylamino)ethyl methacrylate and glycerol monomethacrylate as detailed elsewhere.[36]

Polymer brush fabrication: Silicon blocks were cleaned by initially soaking them for 1 h in a concentrated piranha solution (97% H_2SO_4 and 30% H_2O_2, ratio of 3:1). After rinsing them with an abundance of demineralised water the Si blocks were cleaned with oxygen plasma for 10 min.

To graft a polymer brush to the inherent SiO_2 surface of the Si blocks, an intermediate polystyrene, PS, layer is chemically deposited onto the block's polished surface. This is achieved using the methodology of Maas et al.[37] with a solution containing a 9:1 mixture of the M_w 1,700 and M_w 19,000 vinyl-PS polymers dissolved in chloroform with a concentration of 12 g/L. This solution is poured to completely cover the Si block's surface. The block is then left in a fume hood to allow the chloroform to completely evaporate. Afterwards the block is placed in a vacuum oven for 48 h at 150 ˚C and then left to cool for 8 h under an argon gas environment to covalently bond the vinyl groups to the SiO_2. After cooling, the block is washed with chloroform to remove excess vinyl-PS.

PEO brushes on a silicon block with a grafting density of 0.2 nm^{-2} were prepared based on the method of Currie et al,[38] that was later updated by de Vos et al.[39] In this method, a known quantity of a PS-PEO diblock-copolymer is dissolved in chloroform and applied to the surface of a Langmuir–Blodgett trough to form a sparse PEO brush at the air-water interface, with the hydrophobic PS block anchoring the polymer. The barrier of the trough is then used to concentrate the PS-PEO chains at the air-water interface, providing a direct control over the brush grafting density. When the desired grafting density is reached, the polymers are transferred to a PS coated silicon block by Langmuir-Schaefer (horizontal) dipping. The grafting density at

the air-water interface needs to be higher than the desired grafting density as some polymer is lost during the transfer.[39] The grafting density was confirmed using a dry thickness measurement acquired by ellipsometry.

The polymer brush layers used to confine all the samples were grafted onto the flexible polymer (Melinex®) sheet instead of a silicon block. Initially, a deuterated polystyrene, dPS, layer was deposited onto the Melinex® from chloroform solution (1 g/L) by spin coating at 500 rpm; resulting in a layer that is over 500 nm thick. This is necessary to provide good reflection and contrast in the neutron experiments and to allow easy grafting of the polymer brush to the surface of the Melinex®. The later stretching of the Melinex® to provide confinement is less than the PS yield point in the region of the neutron beam's footprint.

A deuterated poly(ethylene oxide), dPEO, brush was then grafted to the dPS layer using a Langmuir–Blodgett (vertical) dipping method, using a dPS-dPEO diblock-copolymer with the same trough settings as used for the horizontal dipping of the Si blocks. Both dPEO brushes with a brush density of 0.2 nm^{-2} and 0.15 nm^{-2} were created to match the grafting density of the brushes on the Si blocks.

In addition, 3 PDMAEMA polymer brushes were grafted onto silicon blocks by surface-initiated polymerisation with an approximate grafting density of 0.15 nm^{-2}, using an *activators regenerated by electron transfer-atom transfer radical polymerization* (ARGET-ATRP) method,[40] similar to published procedures.[33] Briefly, silicon blocks were washed thoroughly with water, acetone and ethanol before being dried and cleaned by UV/O_3 exposure for at least 30 minutes. Blocks were then immersed in a 1 $mg.ml^{-1}$ solution of a cationic polyelectrolyte macroinitiator[36,41] for approximately 16 hours, washed with water and dried under a nitrogen stream. For ARGET-ATRP polymerisation, blocks were immersed in a deoxygenated solution

containing 30.0 ml propan-2-ol, 30.0 ml 2-(dimethylamino)ethyl-methacrylate (DMAEMA, 28 g, 178 mmol), 1.58 ml water, 16 mg $CuBr_2$ (0.072 mmol), 125 mg ascorbic acid (AA, 0.710 mmol), 82.1 mg 1,1,4,7,10,10-hexamethyltriethylenetetramine (HMTETA, 0.356 mmol) in a nitrogen atmosphere for typically 16 hours (target DMAEMA:Cu:AA:HMTETA mole ratio = 2500:1:10:5). Blocks were then washed with propan-2-ol and water and dried under a nitrogen stream.

A full list of the materials used for these samples and further experimental details can be found in the supporting information.

Neutron Reflectometry Measurements: The neutron reflectometry measurements were conducted at ISIS on the INTER reflectometer,[42] Rutherford-Appleton Lab, UK. The machine was operated in time-of-flight mode with a wavelength range of 0.5 to 16 Å. Measurements were acquired at two grazing angles, 0.3˚ and 1.2˚, resulting in useful statistical reflection data being obtained in the 0.004 to 0.20 $Å^{-1}$ *Q*-range. The instrument's collimating slits were operated with variable openings to maintain a fixed beam footprint of 25 × 25 mm^2 area in the centre of the sample at all incident angles.

The samples were investigated in a neutron reflection confinement cell using a flexible polymer sheet, where full details of this sample environment are described in the article of de Vos et al.[18] However, for the experiments in this article the flexible polymer sheet always had a dPEO brush layer on the side facing the silicon block. The hydrating solution, used to wet the brushes, was dropped onto the silicon block brush prior to increasing the pneumatic pressure of the sample environment to provide contact between each brush pair. For the PDMAEMA brushes, the pH value of this solution (adjusted with HCl and/or NaOH in the presence of 1mM NaCl) is what is described in this work when we refer to the pH.

The resultant data acquired from these experiments were analysed by fitting a multi-layer optical model to the neutron reflectivity curves. Full details of the model used can be found in the supporting information.

Results and Discussion

Confinement of two neutral symmetric brushes: Experiments were initially undertaken using a pair of uncharged polymer brushes fabricated from PEO and its deuterated equivalent, dPEO. These experiments were performed in order to demonstrate that the apparatus is indeed capable of determining the structure of the polymer brushes and that direct and full contact between the brushes can be achieved, without the added complexity of charge. The experimental data acquired, Figure 4, first investigated an unconfined hydrogenated PEO brush, hydrated with H_2O. From fits to the neutron reflectivity data, the expected parabolic profile[10,24,28] for a polymer brush was observed.

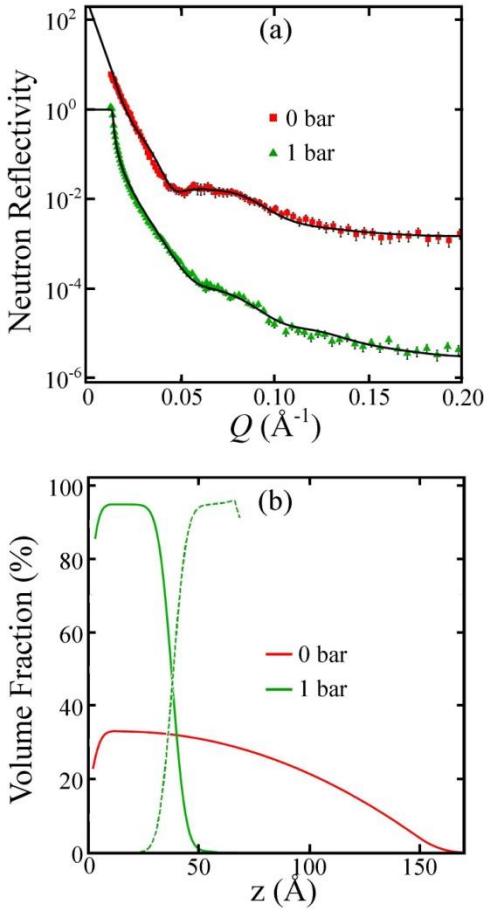

Figure 4: (a) Neutron reflectivity data and fits for a 0.2nm^{-2} PEO brush unconfined (0 bar) and compressed against another 0.2nm^{-2} dPEO brush. Data sets offset for clarity. (b) The volume fraction profiles of each polymer brush derived from the scattering length density profiles used to fit the data in part a, the dashed line indicates the d-PEO brush.

Confinement with a dPEO brush on the polymer sheet allowed the two polymer brushes to be clearly distinguished due to the significant difference in scattering length density between

hydrogenated and deuterated materials. When the confining pressure was raised to 1 bar, the fits to the neutron reflectivity data indicate that both brushes compact into separate polymer blocks with very little overlap of their volume fraction profiles. These results are consistent with the nSCF simulations, demonstrating that steric interactions between the uncharged polymers prevent any meaningful interpenetration. However, there is a discrepancy between the simulations and experimental data in the volume fraction of the polymer blocks. Experimentally, this volume fraction is observed to be >90%, yet the simulations suggest a value nearer 40%. The discrepancy, we believe, is due to nSCF theories overestimating the importance of osmotic pressures in a confined environment, as discussed in a previous article.[21]

These experimental observations of brush compression are similar to those determined by Kuhl et al.;[11,16,17] however, with our improved apparatus, complete contact and compression can be achieved with the results demonstrating that the whole of both brushes will compact almost completely.

Further confinement at higher pressures up to 5 bar, provided in the supporting information, only slightly increased the volume fraction of the compacted polymer blocks and did not affect the degree of interpenetration.

Confinement of asymmetric brushes: To determine the behaviour of a charged brush interacting with an uncharged brush, hydrogenated PDMAEMA was used. This is a weakly charged cationic polyelectrolyte with a pK_a in dilute solution of around 7.5.[33,34] A dPEO brush was compressed with a PDMAEMA brush, with the hydrating solution at different pH values. Figure 5 shows the reflectivity for the three pH levels that were examined. pH values of 2 and 5 were used to measure the interaction between a charged and an uncharged brush. In addition, a pH of 10 was used as a control, since the PDMAEMA will be uncharged at this value and so

little interpenetration is predicted. Although weak polyelectrolyte brushes can also be very sensitive to ionic strength as well as pH, the typical ionic strength changes due to pH adjustment in our experiments have been shown to produce little change in swelling for PDMAEMA brushes.[43] Our experimental focus was thus on more extreme pH values (with respect to the pK_a) to unambiguously show the switch between high and low degrees of interpenetration.

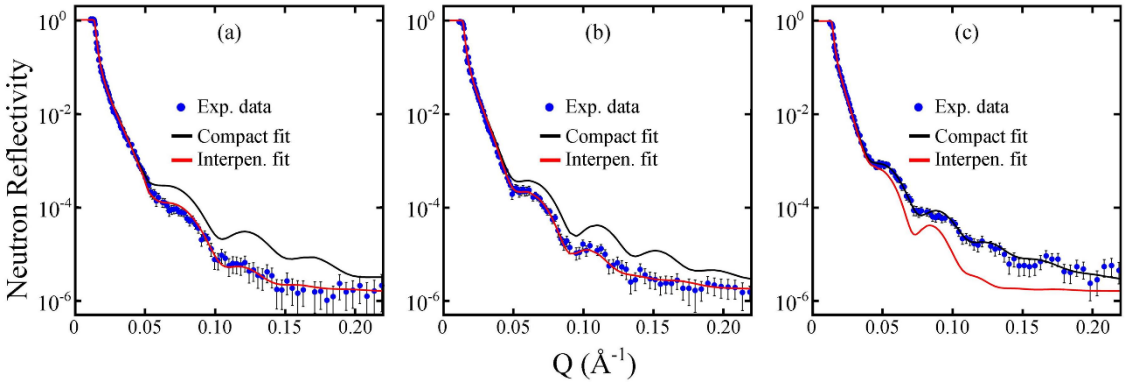

Figure 5: Neutron reflectivity data and potential fits for PDMAEMA and dPEO brushes confined with a pressure of 6 bar when the hydrating solution is (a) pH 2, (b) pH 5 and (c) pH 10. In all parts, a compact and interpenetrating case is presented illustrating the switch between non-interpenetration and interpenetration. The data for each pH were obtained with a separate pair of polymer brushes.

The neutron reflectivity data acquired when the pairs of polymer brushes were compressed together with a pressure of 6 bar are presented in Figure 5. For all cases, the data demonstrate several Kiessig fringes. Therefore, reliable fits about the properties of each layer of the sample can be made using a reflectivity model, described in detail in the supporting information. The presence of these clear fringes indicates that the degree of interpenetration is constant across the sample. If this were not the case, the dispersity (different degrees of interpenetration or brush

thicknesses in different locations of the sample area) would obscure and blur these fringes. An example of the data acquired from an unconfined PDMAEMA brush can also be found in the supporting information.

For each pH examined, two fits to the data are presented. One of the fits is the best fit possible for the scenario predicted by the nSCF theory above: interpenetrating brushes for the pH 2 or 5 data, and a non-interpenetrating, compact, brush profile for the pH 10 data. As a comparison, an additional fit for the opposite case is also presented, where the only change in the reflectivity model is how we consider the interface between the two brushes. It is clear from the two potential fits as to which scenario applies to each data set. The difference in the average signal level for the interpenetrating and compacted cases is because the reflectivity data are dominated by the hydrogenous PDMAEMA. Therefore, the sharp transition in the scattering length density profile of the compact case and the gradual transition for the interpenetrating case, as shown in the supporting information, results in clearly distinct average neutron reflectivity signal levels.

The volume fraction profiles for the brushes that generate the neutron reflectivity fits and are shown in Figure 6. The profiles for the predicted interpenetration case, for each pH, are in qualitative agreement with the profile predicted in the nSCF simulations shown in Figure 1. For the pH 2 and 5 interpenetrating samples, significant overlap is observed between the uncharged dPEO brush and the charged PDMAEMA brush. The PDMAEMA brush also demonstrates the predicted asymmetric behaviour, where the charged PDMAEMA brush is more hydrated than the opposing dPEO brush. Since the dPEO volume fraction is close to 100 % at its grafting interface, we can conclude that all the hydration in the overlap region has been driven by the charged brush. The dashed volume fraction profiles shown in Figure 6 are the volume fraction profiles

used to generate the poor fit in Figure 5, which correspond to the alternative scenario not predicted by the nSCF simulations.

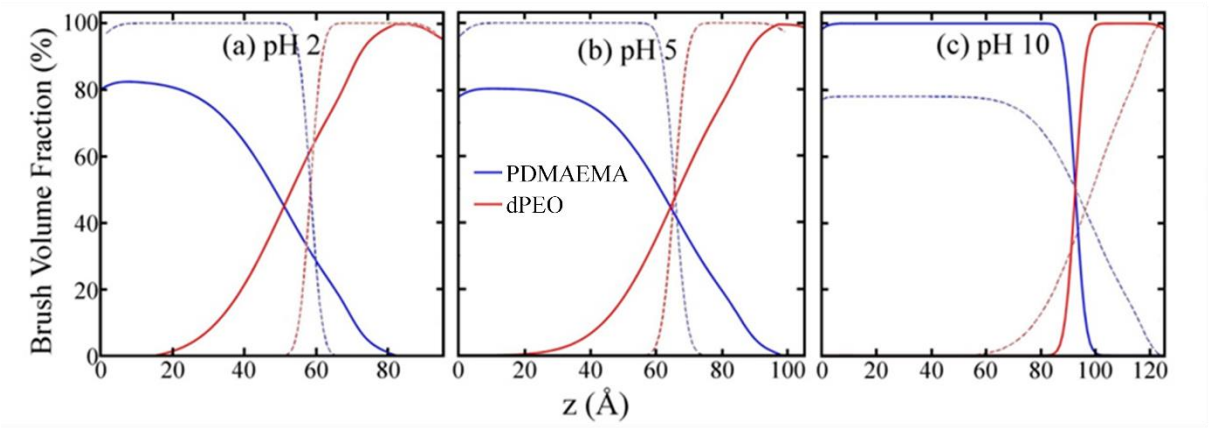

Figure 6: Comparison of the brush volume fraction profiles for (a) pH 2, (b) pH 5 and (c) pH 10. Solid lines are for the fit of the predicted model to the reflectivity data and the dashed lines are a theoretical polymer brush profile for the alternative scenario. The values are derived from scattering length density profiles used to generate the reflectivity shown in figure 4.

It is important to mention here that the density profiles presented in figure 6 and 7, do not represent true equilibrium situations. With just a 5-20% percent remaining water, the chain mobility will be very low, while additionally with so little remaining water the charge of the PDMAEMA chains will be strongly reduced due to proton dissociation or possibly counter ion condensation. This would mean that the degree of overlap is much more determined upon initial contact between the two polymer brushes, when hydration and thus chain mobility is still high, and when the PDAEMA brush is still much more charged. The more hydrated state determining the overlap after further hydration is also in line with our theoretical approach, where the interpenetration occurs at much higher degrees of hydration.

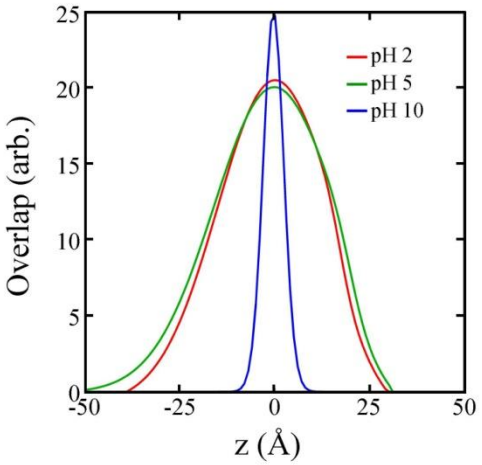

Figure 7: Polymer brush overlap. The product of both polymer brushes' volume fractions (×100) as a function of distance from the intermediate contact point is presented for the best fitting scenario.

An alternative method of comparing the interpenetrating and compacted brush scenarios is to view each pair of brushes' overlap profile, the product of each brush's volume fraction for any given *z* co-ordinate, Figure 7. This figure clearly distinguishes the sharp small physical overlap of the compacted brushes of the pH 10 data set and the broad overlap of the interpenetrating pH 2 and 5 brushes. The lower peak value in Figure 7 for the interpenetrating brushes' overlap profile, compared to the compacted pH 10 profile, is due to the small retention of water with a charged brush lowering the polymer volume fraction profiles of Figure 6, used to calculate the overlap profile. Interestingly, because the hydration is generally associated with the charged brush, this results in the overlap profile for interpenetrating brushes becoming skewed, in contrast to the compacted overlap profile. This suggests that there may be a slightly increased ability of the uncharged brush to penetrate the charged brush.

Interpenetration between polymer brushes is generally considered as the key parameter that determines the friction between two brush decorated surfaces[44]. Naturally there are other parameters, the sliding rate being an important one, but it can be clear that control over brush interpenetration could also lead to control over friction. Here we propose that specifically our system of a PDMAEMA brush combined with a PEO brush, and more generally any combination of a weak polyelectrolyte brush and a neutral brush under aqueous conditions, would lead to a system where the pH of the solution can be used to tune brush interpenetration and thus friction. A very interesting alternative to our approach was recently published by Raftari et al.[45] They studied two weak polyelectrolytes, a polycation and a polyanion, which gave electrostatic attraction around neutral pH leading to very high adhesion and friction forces. At extreme pH values, high and low, much lower frictional forces were observed as under those conditions just one brush was charged, while the other was uncharged, no longer leading to polyelectrolyte complexation.

Conclusions

In conclusion, it has been clearly demonstrated that in the confinement of a weakly charged and an uncharged polymer brush, the brush interpenetration becomes a parameter that can be controlled by the pH of the hydrating solution. Experimentally, this was investigated with a unique combination of a surface force apparatus and neutron reflection, where two polymer brushes were forced into complete contact. If both of these brushes are uncharged, they compress against each other to form polymer blocks. The brushes then have a high volume fraction with very little overlap between them because any interpenetration would require unfavourable stretching of polymer chains.

However, if one of these brushes is charged, through adjusting the pH of the hydrating solution, we observe that the two brushes significantly interpenetrate each other on initial contact. This interpenetration then remains as the brushes de-hydrate and most of the charge groups are also removed. This interpenetration can be understood as a favourable interaction in the system, where the uncharged polymer is used to dilute and increase the separation of the charges when the confining force removes almost all of the water from the system. The only water that remains is likely bound to hydration shells that form around the few charged groups that remain, which is not sufficient to adequately separate the charges in this system so interpenetration of the uncharged brush is favoured. Further de-hydration then locks the polymer chains in place as there is no kinetic process to re-order them in a heavily dehydrated environment.

For both situations, the experimental data were found to agree with the predictions generated by the nSCF simulations with the exception of the amount of hydration retained by polymer brushes under confinement; where this has been extensively discussed elsewhere.[21] The simulations further demonstrate that a very gradual and potentially tuneable change from low to high interpenetration is expected around the pK_a of the polybasic brush.

From our experiments and simulations, we have determined that by adjusting the pH of the solution hydrating polymer brushes we can control their interpenetration. This should prove a significant factor in designing brushes with controllable friction properties.

Acknowledgements

The authors gratefully acknowledge the superb work of Charlie Murray, from the Chemistry workshop and Richard Exley, Adrian Crimp, Tim Newbury and Gideon Hugo from the Physics workshop at the University of Bristol who created our sample environment. In addition, we

would also like to extend our thanks to ISIS, RAL, for allocating beam time for these experiments RB1220242 and RB1310373, as well as the funding provided by EPSRC under Grant EP/H0148611. Yuting Li and Steven Armes are thanked for the synthesis and donation of the cationic macroinitiator.

Supporting Information Available: Additional experimental details, fitting parameters and the scattering length density profiles used to fit the neutron reflectivity data sets presented in this manuscript. This material is available free of charge via the Internet at http://pubs.acs.org.

References

(1) Milner, S. T. Polymer Brushes. *Science* **1991**, *251* (4996), 905–914.
(2) Currie, E. P. K.; Norde, W.; Cohen Stuart, M. A. Tethered Polymer Chains: Surface Chemistry and Their Impact on Colloidal and Surface Properties. *Adv. Colloid Interface Sci.* **2003**, *100-102*, 205–265.
(3) Galuschko, A.; Spirin, L.; Kreer, T.; Johner, A.; Pastorino, C.; Wittmer, J.; Baschnagel, J. Frictional Forces between Strongly Compressed, Nonentangled Polymer Brushes: Molecular Dynamics Simulations and Scaling Theory. *Langmuir* **2010**, *26* (9), 6418–6429.
(4) Murat, M.; Grest, G. Interaction between Grafted Polymeric Brushes: A Molecular-Dynamics Study. *Phys. Rev. Lett.* **1989**, *63* (10), 1074–1077.
(5) Klein, J.; Kumacheva, E.; Mahalu, D.; Perahia, D.; Fetters, L. J. Reduction of Frictional Forces between Solid Surfaces Bearing Polymer Brushes. *Nature* **1994**, *370* (6491), 634–636.
(6) Klein, J. Shear, Friction, and Lubrication Forces Between Polymer-Bearing Surfaces. *Annu. Rev. Mater. Sci.* **1996**, *26* (1), 581–612.
(7) Raviv, U.; Giasson, S.; Kampf, N.; Gohy, J.-F.; Jérôme, R.; Klein, J. Lubrication by Charged Polymers. *Nature* **2003**, *425* (6954), 163–165.
(8) Russano, D.; Carrillo, J.-M. Y.; Dobrynin, A. V. Interaction between Brush Layers of Bottle-Brush Polyelectrolytes: Molecular Dynamics Simulations. *Langmuir* **2011**, *27* (17), 11044–11051.
(9) Ou, Y.; Sokoloff, J. B.; Stevens, M. J. Comparison of the Kinetic Friction of Planar Neutral and Polyelectrolyte Polymer Brushes Using Molecular Dynamics Simulations. *Phys. Rev. E. Stat. Nonlin. Soft Matter Phys.* **2012**, *85* (1 Pt 1), 011801.
(10) Karim, A.; Satija, S.; Douglas, J.; Ankner, J.; Fetters, L. Neutron Reflectivity Study of the Density Profile of a Model End-Grafted Polymer Brush: Influence of Solvent Quality. *Phys. Rev. Lett.* **1994**, *73* (25), 3407–3410.
(11) Elliott, I. G.; Mulder, D. E.; Träskelin, P. T.; Ell, J. R.; Patten, T. E.; Kuhl, T. L.; Faller,

R. Confined Polymer Systems: Synergies between Simulations and Neutron Scattering Experiments. *Soft Matter* **2009**, *5* (23), 4612–4622.
(12) Cosgrove, T.; Luckham, P. F.; Richardson, R. M.; Webster, J. R. P.; Zarbakhsh, A. The Measurement of Volume Fraction Profiles for Adsorbed Polymers under Compression Using Neutron Reflectometry. *Colloids Surfaces A Physicochem. Eng. Asp.* **1994**, *86*, 103–110.
(13) Pasche, S.; Textor, M.; Meagher, L.; Spencer, N. D.; Griesser, H. J. Relationship between Interfacial Forces Measured by Colloid-Probe Atomic Force Microscopy and Protein Resistance of Poly(ethylene Glycol)-Grafted poly(L-Lysine) Adlayers on Niobia Surfaces. *Langmuir* **2005**, *21* (14), 6508–6520.
(14) Thurn-Albrecht, T.; Schotter, J.; Kastle, G. A.; Emley, N.; Shibauchi, T.; Krusin-Elbaum, L.; Guarini, K.; Black, C. T.; Tuominen, M. T.; Russell, T. P. Ultrahigh-Density Nanowire Arrays Grown in Self-Assembled Diblock Copolymer Templates. *Science (80-.).* **2000**, *290* (5499), 2126–2129.
(15) Kellogg, G.; Walton, D.; Mayes, A.; Lambooy, P.; Russell, T.; Gallagher, P.; Satija, S. Observed Surface Energy Effects in Confined Diblock Copolymers. *Phys. Rev. Lett.* **1996**, *76* (14), 2503–2506.
(16) Hamilton, W. A.; Smith, G. S.; Alcantar, N. A.; Majewski, J.; Toomey, R. G.; Kuhl, T. L. Determining the Density Profile of Confined Polymer Brushes with Neutron Reflectivity. *J. Polym. Sci. Part B Polym. Phys.* **2004**, *42* (17), 3290–3301.
(17) Mulder, D. J.; Kuhl, T. L. Polymer Brushes in Restricted Geometries. *Soft Matter* **2010**, *6* (21), 5401.
(18) de Vos, W. M.; Mears, L. L. E.; Richardson, R. M.; Cosgrove, T.; Dalgliesh, R. M.; Prescott, S. W. Measuring the Structure of Thin Soft Matter Films under Confinement: A Surface-Force Type Apparatus for Neutron Reflection, Based on a Flexible Membrane Approach. *Rev. Sci. Instrum.* **2012**, *83* (11), 113903.
(19) Abbott, S. B.; de Vos, W. M.; Mears, L. L. E.; Barker, R.; Richardson, R. M.; Prescott, S. W. Hydration of Odd–Even Terminated Polyelectrolyte Multilayers under Mechanical Confinement. *Macromolecules* **2014**, *47* (10), 3263–3273.
(20) de Vos, W. M.; Mears, L. L. E.; Richardson, R. M.; Cosgrove, T.; Barker, R.; Prescott, S. W. Nonuniform Hydration and Odd–Even Effects in Polyelectrolyte Multilayers under a Confining Pressure. *Macromolecules* **2013**, *46* (3), 1027–1034.
(21) Abbott, S. B.; de Vos, W. M.; Mears, L. L. E.; Cattoz, B.; Skoda, M. W. A.; Barker, R.; Richardson, R. M.; Prescott, S. W. Is Osmotic Pressure Relevant in the Mechanical Confinement of a Polymer Brush? *Macromolecules* **2015**, *48* (7), 150319144329000.
(22) Currie, E. P. K.; Wagemaker, M.; Cohen Stuart, M. A.; van Well, A. A. Structure of Monodisperse and Bimodal Brushes. *Macromolecules* **1999**, *32* (26), 9041–9050.
(23) Murat, M.; Grest, G. S. Structure of a Grafted Polymer Brush: A Molecular Dynamics Simulation. *Macromolecules* **1989**, *22* (10), 4054–4059.
(24) Scheutjens, J. M. H. M.; Fleer, G. J. Statistical Theory of the Adsorption of Interacting Chain Molecules. 1. Partition Function, Segment Density Distribution, and Adsorption Isotherms. *J. Phys. Chem.* **1979**, *83* (12), 1619–1635.
(25) Zhulina, E. B.; Leermakers, F. A. M. A Self-Consistent Field Analysis of the Neurofilament Brush with Amino-Acid Resolution. *Biophys. J.* **2007**, *93* (5), 1421–1430.
(26) Wijmans, C. M.; Scheutjens, J. M. H. M.; Zhulina, E. B. Self-Consistent Field Theories for Polymer Brushes: Lattice Calculations and an Asymptotic Analytical Description.

Macromolecules **1992**, *25* (10), 2657–2665.
(27) Edwards, S. F. The Statistical Mechanics of Polymers with Excluded Volume. *Proc. Phys. Soc.* **1965**, *85* (4), 613–624.
(28) Zhulina, Y. B.; Pryamitsyn, V. A.; Borisov, O. V. Structure and Conformational Transitions in Grafted Polymer Chain Layers. A New Theory. *Polym. Sci. U.S.S.R.* **1989**, *31* (1), 205–216.
(29) Milner, S. T.; Witten, T. A.; Cates, M. E. Theory of the Grafted Polymer Brush. *Macromolecules* **1988**, *21* (8), 2610–2619.
(30) Lyklema, J. *Fundamentals of Interface and Colloid Science. Volume 1: Fundamentals*; Academic Press: London, 1991.
(31) Israels, R.; Scheutjens, J. M. H. M.; Fleer, G. J. Adsorption of Ionic Block Copolymers: Self-Consistent-Field Analysis and Scaling Predictions. *Macromolecules* **1993**, *26* (20), 5405–5413.
(32) Zhulina, E. B.; Borisov, O. V. Structure and Interaction of Weakly Charged Polyelectrolyte Brushes: Self-Consistent Field Theory. *J. Chem. Phys.* **1997**, *107* (15), 5952.
(33) Willott, J. D.; Humphreys, B. A.; Murdoch, T. J.; Edmondson, S.; Webber, G. B.; Wanless, E. J. Hydrophobic Effects within the Dynamic pH-Response of Polybasic Tertiary Amine Methacrylate Brushes. *Phys. Chem. Chem. Phys.* **2015**, *17* (5), 3880–3890.
(34) Layman, J. M.; Ramirez, S. M.; Green, M. D.; Long, T. E. Influence of Polycation Molecular Weight on poly(2-Dimethylaminoethyl Methacrylate)-Mediated DNA Delivery in Vitro. *Biomacromolecules* **2009**, *10* (5), 1244–1252.
(35) Lyatskaya, Y. V.; Leermakers, F. A. M.; Fleer, G. J.; Zhulina, E. B.; Birshtein, T. M. Analytical Self-Consistent-Field Model of Weak Polyacid Brushes. *Macromolecules* **1995**, *28* (10), 3562–3569.
(36) Willott, J. D.; Murdoch, T. J.; Humphreys, B. A.; Edmondson, S.; Webber, G. B.; Wanless, E. J. Critical Salt Effects in the Swelling Behavior of a Weak Polybasic Brush. *Langmuir* **2014**, *30* (7), 1827–1836.
(37) Maas, J. H.; Cohen Stuart, M. A.; Sieval, A. B.; Zuilhof, H.; Sudhölter, E. J. R. Preparation of Polystyrene Brushes by Reaction of Terminal Vinyl Groups on Silicon and Silica Surfaces. *Thin Solid Films* **2003**, *426* (1-2), 135–139.
(38) Currie, E. P. .; Wagemaker, M.; Stuart, M. A. C.; van Well, A. . Structure of Grafted Polymers, Investigated with Neutron Reflectometry. *Phys. B Condens. Matter* **2000**, *283* (1-3), 17–21.
(39) de Vos, W. M.; de Keizer, A.; Kleijn, J. M.; Cohen Stuart, M. A. The Production of PEO Polymer Brushes via Langmuir-Blodgett and Langmuir-Schaeffer Methods: Incomplete Transfer and Its Consequences. *Langmuir* **2009**, *25* (8), 4490–4497.
(40) Matyjaszewski, K.; Dong, H.; Jakubowski, W.; Pietrasik, J.; Kusumo, A. Grafting from Surfaces For "everyone": ARGET ATRP in the Presence of Air. *Langmuir* **2007**, *23* (8), 4528–4531.
(41) Chen, X. Y.; Armes, S. P.; Greaves, S. J.; Watts, J. F. Synthesis of Hydrophilic Polymer-Grafted Ultrafine Inorganic Oxide Particles in Protic Media at Ambient Temperature via Atom Transfer Radical Polymerization: Use of an Electrostatically Adsorbed Polyelectrolytic Macroinitiator. *Langmuir* **2004**, *20* (3), 587–595.
(42) Webster, J.; Holt, S.; Dalgliesh, R. INTER the Chemical Interfaces Reflectometer on

Target Station 2 at ISIS. *Phys. B Condens. Matter* **2006**, *385-386*, 1164–1166.
(43) Willott, J. D.; Murdoch, T. J.; Humphreys, B. A.; Edmondson, S.; Wanless, E. J.; Webber, G. B. Anion-Specific Effects on the Behavior of pH-Sensitive Polybasic Brushes. *Langmuir* **2015**, *31* (12), 3707–3717.
(44) Kreer, T. Polymer-Brush Lubrication: A Review of Recent Theoretical Advances. *Soft Matter* **2016**, *12* (15), 3479–3501.
(45) Raftari, M.; Zhang, Z. J.; Carter, S. R.; Leggett, G. J.; Geoghegan, M. Nanoscale Contact Mechanics between Two Grafted Polyelectrolyte Surfaces. *Macromolecules* **2015**, *48* (17), 6272–6279.

Table of Contents Graphic

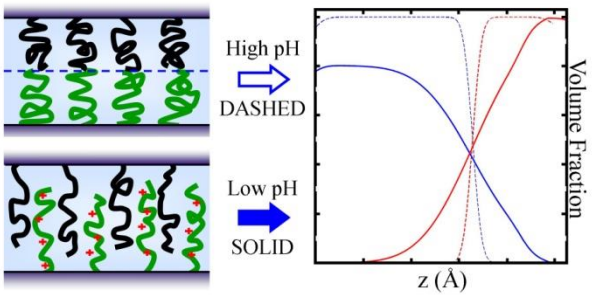

Supporting Information:

Switching the Interpenetration of Confined Asymmetric Polymer Brushes.

Stephen B. Abbott,[a,b] Wiebe M. de Vos,[*,c] Laura L. E. Mears,[a] Maximilian Skoda,[d] Robert Dalgliesh,[d] Steve Edmondson,[e] Robert M. Richardson,[a] Stuart W. Prescott[b,f]

Further experimental details

PDMAEMA Brush Formation: For ARGET-ATRP polymerisation, 30.0 ml propan-2-ol, 30.0 ml 2-(dimethylamino)ethyl-methacrylate (DMAEMA, 28 g, 178 mmol), 82.1 mg 1,1,4,7,10,10-hexamethyltriethylenetetramine (HMTETA, 0.356 mmol) and 1.58 ml water were first mixed in a round-bottomed flask sealed with a septum and deoxygenated by bubbling through nitrogen for at least 15 minutes. 16 mg $CuBr_2$ (0.072 mmol) and 125 mg ascorbic acid (AA, 0.710 mmol) were then added, the headspace purged with nitrogen and the mixture magnetically stirred and briefly sonicated to dissolve the solids. A very light yellow solution resulted. Meanwhile, a silicon block was placed in a beaker which was sealed inside a vacuum desiccator. The desiccator was filled with nitrogen using at least three pump/refill cycles. The polymerisation solution was then syringed over the silicon block. After the desired polymerisation time, typically 16 hours, the block was removed from the desiccators. The sample block was then washed with propan-2-ol and again with water, afterwards the sample was dried under a nitrogen stream.

Data Analysis: Fitting of the neutron reflectivity data was achieved using an optical matrix method[2] in RasCAL.[3] A custom model was developed for analysing the sample, whereby the unconfined polymer brush is split into 4 layers. A sub-phase and an incident medium are also required. Each of these regions is described by a thickness, roughness and scattering length density (SLD) parameter. In addition, the brush layer also requires a parameter for the water volume fraction.

The incident medium in this model is always a semi-infinite silicon layer, i.e. it only has one boundary interface in the optical calculations. The material of the sub-phase depends on the

confinement and which polymer brush is being analysed. For unconfined PEO brushes, the sub-phase is considered to be a semi-infinite layer of H_2O. When PDMAEMA brushes are examined the sub-phase is a semi-infinite D_2O layer. The SLD of each of these materials is listed in Table S1, unless noted otherwise these values were determined by fitting this model to the experimental data.

Between the incident and sub-phase regions are the layers of the polymer brush sample. The first layer required is to represent a thin SiO_2 layer present on the Si block; the SLD listed in Table S1 is lower than the SLD for pure SiO_2 due to its porosity. A second layer is then required to account for the PS intermediate layer necessary to graft a polymer brush to the substrate. The thicknesses of these layers are determined by ellipsometry measurements between the samples' fabrication stages. The roughness values are determined by fitting the unconfined sample data.

After grafting the brushes to the PS, only a single additional layer is required to describe the additional polymer. The PS component of the co-polymer used to make the brushes is indistinguishable from the PS intermediate layer. Therefore, to account for it, the thickness of the PS intermediate layer, which was determined by ellipsometry, is increased by 15 Å; the expected thickness of the PS component of the brush based on the brush's grafting density, this is approximately the thickness of a single PS monolayer. The thickness of the additional layer used to describe the brush is determined by ellipsometry measurements of a dry sample. The key model parameter is the hydration of this polymer brush layer. The uptake of water both swells the layer's thickness and alters its SLD. The SLD (s) and thickness (δ) of a wet layer are those used in the fitting model. The wet and dry values are related by:

$$s = s_{H_2O}\phi + s_p(1-\phi) \quad \text{(S1)}$$

$$\delta_{wet} = \delta_{dry}/(1-\phi) \quad \text{(S2)}$$

where s_{H_2O} is the SLD of H_2O, s_p is the SLD of the polymer, and ϕ is the volume fraction of the water in the layer (often referred to as hydration).

With this model there are 4 free fitting parameters for unconfined brush data sets, the 3 internal roughnesses and the brush hydration. To account for the rough interfaces in the model, a Gauss error function is used with the roughness parameter listed as the value used to scale this function appropriately. However, the exception to this is the roughness of an unconfined polymer brush, which is modelled using a parabolic function, $1\text{-}ax^2$. To more easily compare the brush's parabolic profile to the sample's internal roughness's, an equivalent Gauss error function value that closely estimates the parabolic shape of the brush is instead provided in Table S2. No dispersity in thickness of any layer of the sample is required to match the experimental data. Compression of the brush significantly alters the roughness and hydration of the brush layer.

When confined, an additional layer is added in order to model the presence of the confining brush. This layer represents the dPEO brush, and the material of the sub-phase is changed to dPS to account for the >50 nm layer deposited onto the Melinex® sheet and the dPS component of the co-polymer used to fabricate the brush. The comparatively large thickness of the dPS means we

can consider this layer to be semi-infinite. The value for the thickness of the dPEO layer was determined from the thickness obtained from previous work with brushes fabricated in the same way with equivalent grafting densities.[4] The thickness of the brushes on the Melinex® cannot be determined directly by ellipsometry due to the transparent nature of the materials and their comparative thicknesses.

The effect of confinement on the brushes depends on whether a sample has charged groups on one of the brushes. Without charged groups only the hydration of the two brushes and the roughness between them are variables, the thicknesses of the layers are not altered and the remaining internal roughness values are kept constant from the unconfined data. Hence there are 3 free parameters for these data sets. If a charged group is present on one of the brushes in the sample then an additional variable needs to be introduced representing the thickness reduction of the sample due to interpenetration. The interpenetration value, *i*, reduces the thickness of both the dPEO and PDMAEMA layers by *i*/2. Interpenetrating samples also have a much higher roughness at the interface of the two brushes. Therefore, there are 4 free parameters for interpenetrating samples. The values used for all these parameters are listed in Table S2.

Using error analysis within the program to calculate the standard deviation error, the uncertainty in the polymer brushes' water volume fraction is ±4% v/v when unconfined and is ±1.5% v/v when confined. The error in the fitted roughness values is ±1 Å.

References

(1) Willott, J. D.; Murdoch, T. J.; Humphreys, B. A.; Edmondson, S.; Webber, G. B.; Wanless, E. J. *Langmuir* **2014**, *30* (7), 1827–1836.

(2) Born, M.; Wolf, E. *Principles of optics*; Pergamon Press: Oxford, UK, 1970.

(3) Hughes, A. RasCAL http://sourceforge.net/projects/rscl/.

(4) Abbott, S. B.; de Vos, W. M.; Mears, L. L. E.; Cattoz, B.; Skoda, M. W. A.; Barker, R.; Richardson, R. M.; Prescott, S. W. *Macromolecules* **2015**, *48* (7), 150319144329000.

Neutron reflectivity model parameters

Table S1: Scattering Length Density (SLD) Values

Material	SLD ($\times 10^{-6}$ Å^{-2})	Material	SLD ($\times 10^{-6}$ Å^{-2})
Si	2.07*	d-PEO	5.70
SiO_2	2.75	d-PS	6.0
Initiator	1.128	H_2O	- 0.56*
PDMAEMA	1.33		

*value determined theoretically†

†Sears, V. F., *Neutron News*, **1992**, *3*, 26-37.

Table S2: Layer Parameters

pH	SiO_2 thickness	SiO_2 roughness	Initiator thickness	Initiator roughness
2	25 Å	4 Å	60 Å	4 Å
5	36 Å	4 Å	65 Å	4 Å
10	35 Å	8 Å	65 Å	4 Å

pH	PDMAEMA dry thickness	PDMAEMA roughness	PDMAEMA hydration	dPEO thickness
2	61 Å	16 Å	19 %	35 Å
5	67 Å	16 Å	20 %	34 Å
10	97 Å	3 Å	0 %	34 Å

pH	dPEO roughness	dPEO hydration	Interpenetration, *i*	Dispersity
2	3 Å	0 %	34 Å	±5 %
5	4 Å	1 %	27 Å	±5 %
10	3 Å	0 %	0 Å	±5 %

Only the values for the interpenetrating (pH2 and pH5) or compact (pH10) case are presented.

Scattering Length Density (SLD) profiles

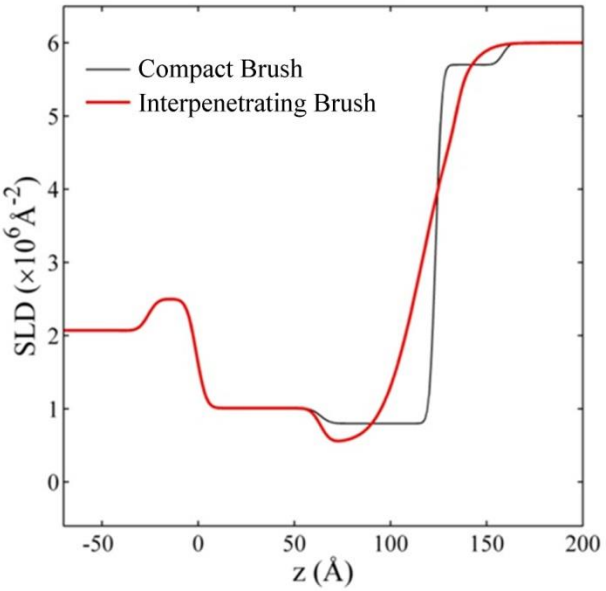

Figure S1: SLD profiles for the pH 2 neutron reflectivity data. The origin (z=0) is at the SiO_2-PS interface. The thick red line is the profile for an interpenetrating brush that results in the ideal fit. The thin black line is the alternative compact profile that results in a poor fit.

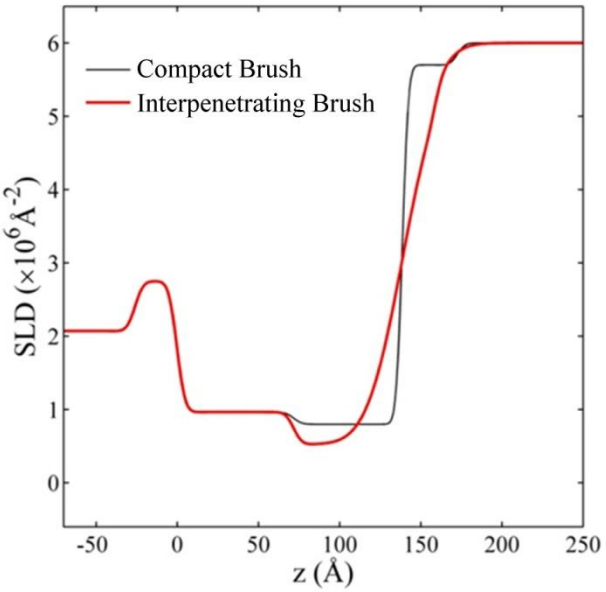

Figure S2: SLD profiles for the pH 5 neutron reflectivity data. The origin (z=0) is at the SiO_2-PS interface. The thick red line is the profile for an interpenetrating brush that results in the ideal fit. The thin black line is the alternative compact profile that results in a poor fit.

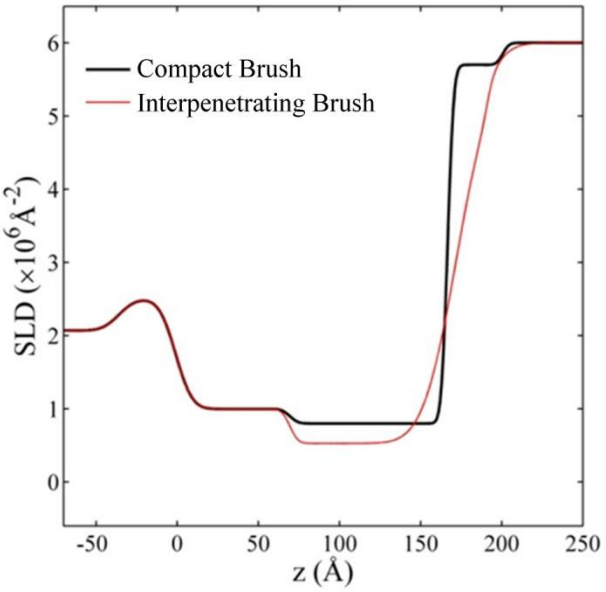

Figure S3: SLD profiles for the pH 10 neutron reflectivity data. The origin (z=0) is at the SiO_2-PS interface. The thick black line is the profile for a compact brush that results in the ideal fit. The thin red line is the alternative interpenetrating profile that results in a poor fit.

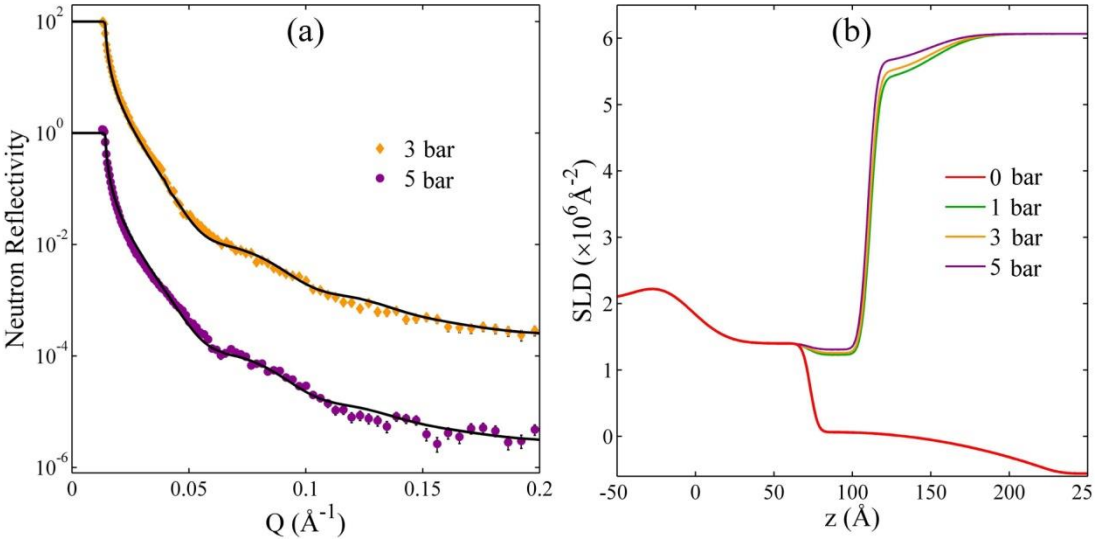

Figure S4: (a) Neutron reflectivity data and fits for the 0.2nm^{-2} d-PEO brush confined at higher pressures. (b) SLD profiles for all the 0.2nm^{-2} PEO:d-PEO neutron reflectivity data. The origin (z=0) is at the SiO_2-PS interface. The majority of the compression occurs with the application of 1 bar, further pressure increases have minimal additional effect.

Unconfined PDMAEMA

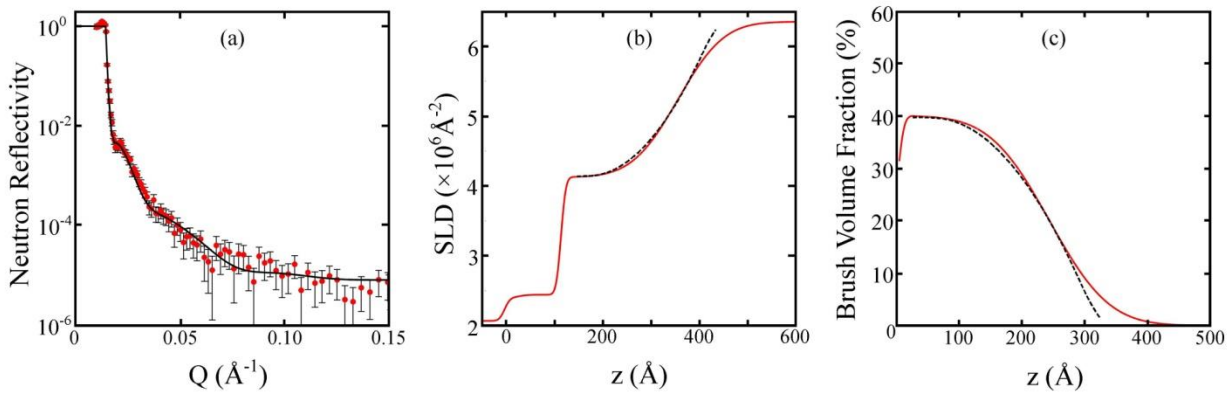

Figure S5: (a) Experimental neutron reflection data for an unconfined PDMAEMA brush hydrated with D_2O. The black line is a fit generated from optical calculations using the SLD profile presented in (b). This results in a volume fraction distribution presented in (c). In both (b) and (c) the black dashed line demonstrates the parabolic like profile of the brush, $1-(3.15\times10^{-5}\ z^2)$. At higher z, at the end of the brush, the volume fraction deviates from the parabolic profile due to the highly dispersed polymer chain length for a brush made by ATRP.

Alternative Plots of Neutron Reflectivity Fits

This figure has the neutron reflectivity multiplied by Q^4, and then plotted on a log-log axis. This removes the Q^4 bias from the plot presented in the main manuscript.

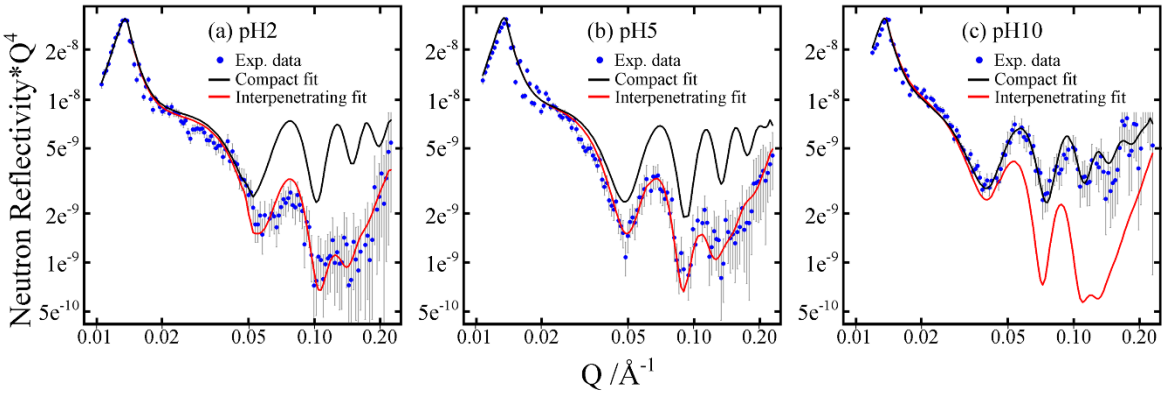

Figure S6: Neutron reflectivity data and potential fits for PDMAEMA and dPEO brushes confined with a pressure of 6 bar when the hydrating solution is (a) pH 2, (b) pH 5 and (c) pH 10. Both a compact and interpenetrating case is presented to illustrating the clear difference in the fit between non-interpenetration and interpenetration.